Electroexcitation of 8^{-} states in^{52}Cr

de Jager, C.W.; de Vries, H.; Fagg, L.W.; Geesaman, D.F.; Karban, O.; Lawson, R.D.; Lindgren, R.A.; Maruyama, X.K.; Morrison, G.C.; Offermann, E.A.J.M.; Sober, D.I.; van Hienen, J.F.A.; Zeidman, B.

published in
Default journal
1988

document version
Publisher's PDF, also known as Version of record

Electroexcitation of 8^- states in ^{52}Cr

D. I. Sober and L. W. Fagg
The Catholic University of America, Washington, D.C. 20064

B. Zeidman, R. D. Lawson, and D. F. Geesaman
Argonne National Laboratory, Argonne, Illinois 60439

G. C. Morrison and O. Karban
University of Birmingham, Birmingham, United Kingdom

X. K. Maruyama*
National Bureau of Standards, Gaithersburg, Maryland 20899

H. de Vries, E. A. J. M. Offermann, and C. W. de Jager
Sektie Kernfysica, Nationaal Instituut voor Kernfysica en Hoge-Energiefysica, 1009 AJ Amsterdam, The Netherlands

R. A. Lindgren
University of Virginia, Charlottesville, Virginia 22901

J. F. A. van Hienen†
Vrije Universiteit, 1007 MC Amsterdam, The Netherlands
(Received 29 February 1988)

Inelastic electron scattering at incident energies between 170 and 260 MeV was used to identify and study $M8$ transitions in ^{52}Cr. A strong transition to an 8^- state at $E_x = 15.47$ MeV was observed, as well as a number of weaker transitions. The results are compared with a single particle-hole shell model calculation that uses a model space of the form $[(f_{7/2})^{11} \times g_{9/2}]_{8^-}$. The shell model calculation and systematics in neighboring nuclei were used to determine the isospin of the observed states. The experimentally determined strengths exhaust 60.8% and 34.5% of the $T=3$ and $T=2$ sum rules, respectively.

I. INTRODUCTION

The study of high-spin "stretched" states, i.e., states reached by excitations of the highest multipolarity that can be attained in a single-particle transition between adjacent major shells, has been a focus of much recent work in electron and hadron scattering. Specifically, in an even-even nucleus a stretched state of angular momentum $J_{\max}$ is reached by a single-particle transition $j_b \rightarrow j_a$, where $j_b = (l_b + \frac{1}{2})$ is the largest single-particle angular momentum in the valence shell, $j_a = (l_a + \frac{1}{2})$ is the largest angular momentum in the next higher shell, and $J_{\max} = j_a + j_b$.

The importance of studying transitions to stretched states arises from the simplicity of the operator governing their excitation. If one neglects $E \geq 3\hbar\omega$ configurations in the wave functions, there is only one single-particle operator which can induce the transition. Second, since $(l_a + l_b) = (J_{\max} - 1)$, the contribution of the orbital part of the magnetic operator vanishes[1] and only the spin contribution remains. As a result, electron, nucleon, and pion scattering cross sections depend upon a common spin transition density, even though the proton and neutron parts of this transition density exhibit different responses to the various probes. With a combination of experiments, this selective response makes it possible to separate isoscalar and isovector components, or alternatively, proton and neutron contributions, so as to provide stringent tests of nuclear wave functions and the structure of the underlying interaction involved in the excitation of stretched transitions.

For p-, sd-, and fp-shell, $J = 0^+$ nuclei, stretched transitions lead to 4^-, 6^-, and 8^- states, respectively. In inelastic electron scattering these states are reached by magnetic transitions which are conveniently studied at backward angles ($> 140°$) and intermediate energies (100–300 MeV). Several substantial reviews of the study of stretched states excited by (e,e'), (p,p'), and (π,π'), in nuclei from ^{12}C to ^{208}Pb, have appeared recently.[2–6] The observed total strength of transitions to these states is typically from 10% to 60% of that predicted by the extreme single-particle-hole model (ESPHM), i.e., by calculation of the transition $(j_b)^n \rightarrow [(j_b)^{n-1} \times j_a]_{J_{\max}}$. Many mechanisms have been proposed to account for this quenching, as well as for the quenching observed in isovector spin-flip excitations of lower multipolarity.[7–10]

Recent measurements have been made of 8^- excitations in ^{54}Fe by electron scattering[11] and pion scatter-

ing.[12] The data from the two experiments in conjunction allowed a decomposition of the isovector and isoscalar spin-flip strengths and provided insight into the systematics of the quenching in the two isospin channels.

A study of the neighboring nucleus ^{52}Cr is of particular interest because it allows a direct approach for investigation of the mechanism of quenching. In addition to the inelastic scattering of various probes, 8^- states can be studied with particle transfer reactions such as ^{51}V(^{3}He,d)^{52}Cr or ^{51}V(α,t)^{52}Cr. Indeed, studies of the inverse[13] reaction, ^{52}Cr(d,^{3}He)^{51}V, together with electron elastic scattering studies of magnetization densities[14] in odd nuclei, strongly suggest that the ^{51}V ground state consists of an almost pure $f_{7/2}$ proton hole in a ^{52}Cr core. This implies that the $g_{9/2}$ proton component of the 8^- states in ^{52}Cr is directly related to proton transfer on ^{51}V, within this simple description of the excitation of the stretched configuration. The different isospin contributions in inelastic scattering of several probes can be used to deduce spectroscopic strengths for comparison with the proton transfer spectroscopic factors for the transitions. Thus, the combined study of all the different reactions may shed light on hitherto obscure details of the mechanism of quenching.

Consequently, an investigation of stretched 8^- excitations in ^{52}Cr, including measurements with several different probes, was initiated. We report here the measurement of $M8$ strength in electron scattering from ^{52}Cr and compare it with the results of a shell model calculation. In Sec. II, a description of the experimental procedure is given. Section III describes the extraction of spectroscopic strengths from the experimental data. Section IV contains a summary of the experimental results, followed by a description of the shell model calculation in Sec. V, and its comparison with the data in Sec. VI. Our conclusions are presented in Sec. VII.

II. EXPERIMENT PROCEDURE

Measurements were performed with the use of the high-resolution quadrupole-dipole-dipole (QDD) spectrometer at the Sektie Kernfysica, National Instituut voor Kernfysica en Hoge-Energie fysica (NIKHEF-K) electron linear accelerator,[15] MEA, in Amsterdam. Two targets were used in this study. The first was a natural Cr foil (83.79% ^{52}Cr) of thickness 20.3 mg/cm^2, which was oriented in transmission geometry. The second was a 99.87%-enriched separated ^{52}Cr target of thickness 17.0 mg/cm^2, which, because of its smaller size, was mounted in reflection geometry.

At the maximum scattering angle at 154°, where most of the data were taken, the 77° (relative to the normal) inclination of the natural Cr target resulted in a counting rate nearly a factor of 4 higher than that obtained from the enriched ^{52}Cr target. Comparable energy straggling contributions were obtained from both targets. The en-

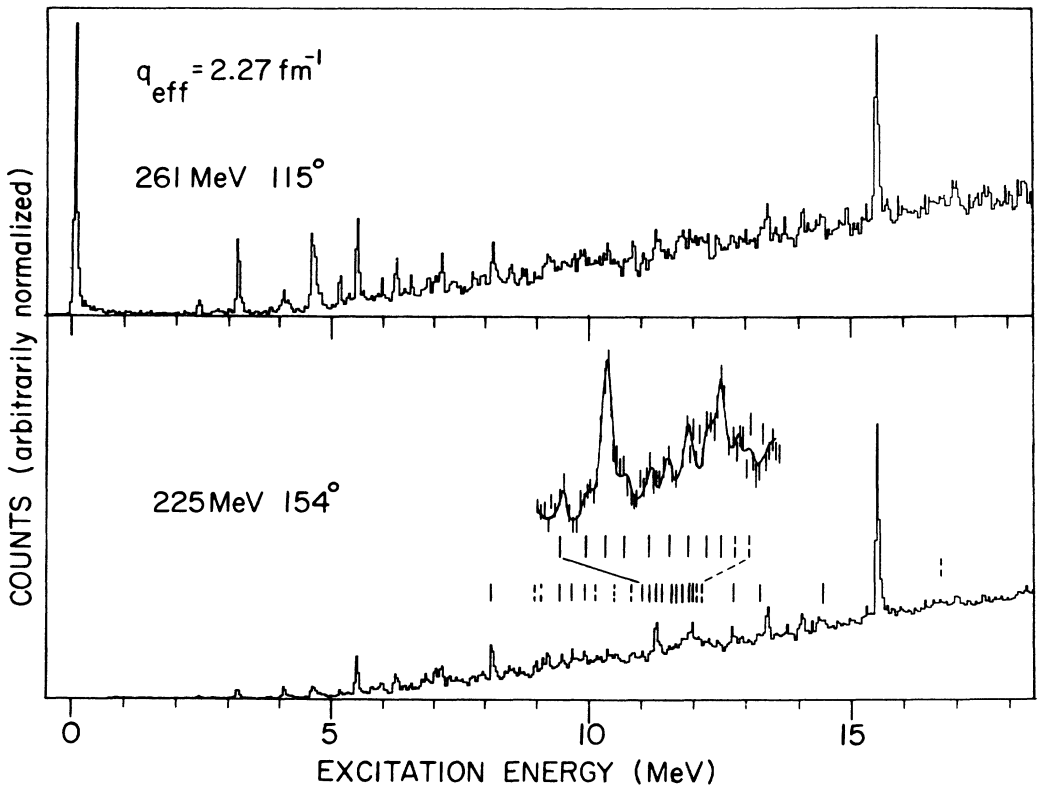

FIG. 1. Spectra measured at 115° and 154° with a natural Cr target. The two spectra correspond to the same value of effective momentum transfer. The vertical lines indicate the locations of the $T=2$ $M8$ excitations identified in this experiment; the dashed lines indicate levels whose $M8$ identification is uncertain. An expanded portion ($\sim$11–12 MeV excitation) of the 154° data spectrum together with output of the peak-fitting routine is also shown.

riched ^{52}Cr target was required in order to prevent misidentification of weak peaks that were due to strong transitions from less abundant Cr isotopes present in the natural Cr target. However, no strong transverse excitations due to the other isotopes were found.

A total of ten data runs were taken: six with the natural Cr target and four with the enriched ^{52}Cr target. Cross sections obtained from measurements on the two targets agreed to better than 5%. At a scattering angle of 154°, cross sections were measured at energies of 170, 200, 225, and 261 MeV corresponding to momentum transfers 1.72, 2.02, 2.27, and 2.61 fm^{-1}, respectively. To allow discrimination between longitudinal and transverse transitions, at an incident energy of 261 MeV data were also obtained at 96° and 115°, angles corresponding to momentum transfers of 2.02 fm^{-1} and 2.27 fm^{-1}, respectively. With the 10% momentum acceptance of the spectrometer, a single magnetic field setting was sufficient to include excitation energies between 2 and 17 MeV at all incident electron energies. Shown in Fig. 1 are spectra obtained at 154° and 115° for a momentum transfer of 2.27 fm^{-1}. The strong selectivity of the backward-angle measurements for magnetic transitions is apparent.

The incident electron energy and the excitation energy calibration of the spectrometer were both determined precisely by a fit to the peak positions of well-established low-lying levels[16] in ^{52}Cr, and to known levels in ^{11}B and ^{14}N measured with a boron nitride target at the same energies and angles. In the final analysis of the ^{52}Cr data, excitation energies up to 16 MeV are determined to better than 0.02 MeV.

Corrections for the efficiency of the focal plane detector system were small and made during the process of sorting the data into equal-sized momentum bins. The normalization was checked by comparing the cross sections of the elastic and low-lying inelastic peaks with those obtained in a previous experiment.[17] The agreement was good to better than 5%.

The momentum-sorted spectra were fitted by a peak-fitting program using a line-shape parametrization.[18] The line shape used was a Gaussian function with symmetric and asymmetric distortions, and a radiative tail function based on the Schwinger term plus empirical corrections. The peak parameters were fitted to a few prominent peaks in each region of the spectrum, and then applied to all peaks in that region with only the height and position varied. The fitted Gaussian widths were between 50 and 80 keV FWHM, consistent with the target thickness and spectrometer resolution. An empirical continuous background function was also fitted to the data.

For the peaks that appeared in two or more spectra, a list of common excitation energies was compiled, and the spectra were refitted with all peaks included in order to obtain a consistent set of peak areas or upper limits. From the yields determined in the final fits, the experimental form factors were calculated for some 90 levels with excitation energies between 2 and 17 MeV.

III. DATA ANALYSIS

The differential cross section for the scattering of electrons from a nucleus is given by

$$d\sigma/d\Omega=(\sigma_M/\eta)(q_\mu^2/q^2)^2F^2(q)$$
$$=\sigma_M/\eta\left[(q_\mu^2/q^2)^2F_L^2(q)+\frac{1}{\epsilon}F_T^2(q)\right], \quad (1)$$

where the nuclear structure information is contained in the squares of the longitudinal and transverse form factors, F_L^2 and F_T^2, respectively. The Mott scattering cross section σ_M, the nuclear recoil factor η, and the virtual photon polarization ϵ, are given by

$$\sigma_M=Z^2\alpha^2\cos^2(\theta/2)/[4E_0^2\sin^4(\theta/2)], \quad (2)$$

$$\eta=1+2(E_0/M)\sin^2(\theta/2), \quad (3)$$

$$1/\epsilon=q_\mu^2/2q^2+\tan^2(\theta/2), \quad (4)$$

where Z is the atomic number of the target nucleus, E_0 is the incident energy, θ is the laboratory scattering angle, M is the mass of the target nucleus, and q and q_μ are the three- and four-momentum transfers, respectively.

In order to relate the measured cross section to theoretical calculations, we corrected for the distortion of the incident electron wave function by the nuclear Coulomb field by replacing q in Eq. (1) with the effective momentum transfer $q_{\rm eff}$ given by

$$q_{\rm eff}=q\left[1+\frac{3}{2}\frac{Z\alpha\hbar c}{E_0R}\right], \quad (5)$$

where

$$R=(\tfrac{5}{3}\langle r^2\rangle)^{1/2}$$

and

$$\langle r^2\rangle^{1/2}=3.643\ \text{fm},$$

the rms radius[17] of the ground-state charge distribution of ^{52}Cr.

In order to distinguish the transverse components from the longitudinal, pairs of cross section measurements were made at different scattering angles (96° and 154°, or 115° and 154°) at the same momentum transfer. From these data, transverse excitations can be identified by a zero vertical intercept on a Rosenbluth plot, which is constructed by plotting $F^2(q)$ vs $1/\epsilon$. As an equivalent procedure to identify transverse transitions, we calculated the quantity

$$\tilde{F}^2(q_{\rm eff},\theta)=\epsilon\eta(d\sigma/d\Omega)/\sigma_M \quad (6)$$

and plotted it vs $q_{\rm eff}$ for all measurements of a single transition. For transverse excitations, the values of $\tilde{F}^2$ measured at equal $q_{\rm eff}$ but different scattering angles must agree, while for longitudinal excitations the values measured at 96° and 115° should exceed those measured at 154° by factors of 11.0 and 6.5, respectively. Figure 2 shows the results for a longitudinal excitation, while several transverse excitations are displayed in Fig. 3. As is seen in Fig. 3, agreement between the forward-angle and 154° measurements of the weaker levels was not always perfect, in part because the radiative tail and density of states observed at the forward angles make it more difficult to extract the cross sections. Levels for which

the values of $\tilde{F}^2$ measured at 96° and 115° agreed with the corresponding 154° measurement to within two standard deviations were accepted as being transverse.

At excitation energies above 5 MeV, only a few levels were clearly identified as purely longitudinal excitations. The majority of those rejected as nontransverse were weakly excited states whose angular distributions were ambiguous, probably because of unresolved mixtures of longitudinal and transverse excitations. No attempt was made to separate the two contributions. It was assumed that the transitions found to be transverse were magnetic with no measurable transverse electric contribution.

For each transition that was identified as magnetic, the q dependence of the extracted form factor was compared to theoretical form factors for several possible magnetic multipoles. These were calculated with harmonic oscillator wave functions assuming reasonable single-particle-hole transition configurations. The form factors were calculated in plane-wave Born approximation, using a computer program based on the code MICRODENS,[19] including corrections for nucleon finite-size and center-of-mass motion.

In the oscillator shell model, the form factor for a stretched magnetic excitation depends on only three parameters: the oscillator parameter b and the neutron and proton spectroscopic strengths Z_n and Z_p. For a pure isovector transition $Z_p = -Z_n$, so that F_T^2 is proportional to $(\mu_n - \mu_p)^2$ and depends on only two parameters: b and $Z_1 = (Z_n - Z_p)/\sqrt{2}$. The oscillator length parameter b depends on the mass number A, approximately as $b \simeq A^{1/6}$ fm. An explicit expression for the form factor is given in Ref. 3. It has the approximate form

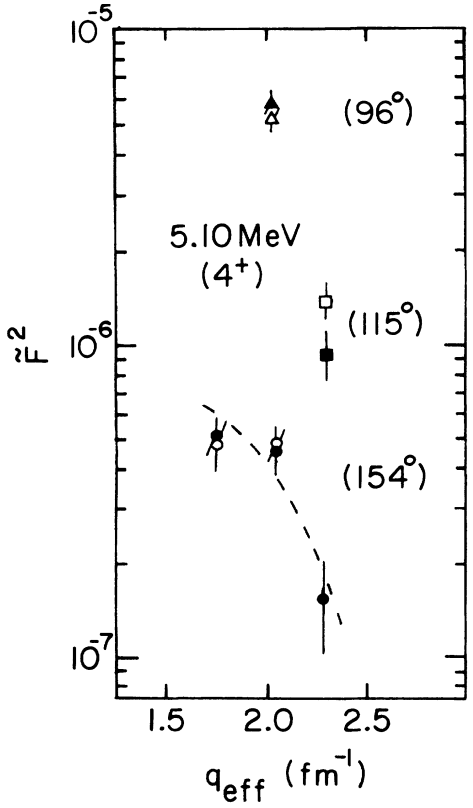

FIG. 2. Transverse form factor squared, extracted from the data under the hypothesis that the transition is transverse, versus effective momentum transfer. The circles indicate measurements at 154°, the squares 115°, and the triangles 96°. Open symbols denote measurements with the natural Cr target, and solid symbols measurements with the separated ^{52}Cr target. The curve through the 154° points for the longitudinal excitation at 5.10 MeV is intended only to guide the eye; note the deviations for the 96° and 115° data.

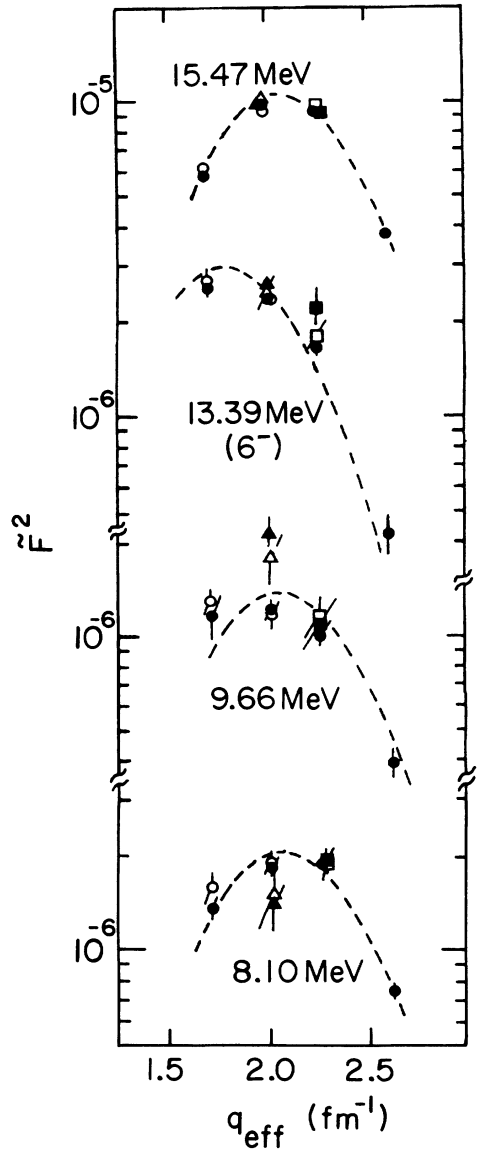

FIG. 3. Transverse form factor squared, extracted from the data under the hypothesis that the transition is transverse, vs effective momentum transfer. The circles indicate measurements at 154°, the squares 115°, and the triangles 96°. Open symbols denote measurements with the natural Cr target, and solid symbols measurements with the separated ^{52}Cr target. The curves for the 8.10, 9.66, and 15.47 MeV levels are $M8$ form factors calculated with $b = 1.86$ fm. The curve for 13.39 MeV is an $M6$ form factor.

TABLE I. Results of fits of F_T^2 for the $E_x = 15.47$ MeV level to various single-particle-hole transitions in the harmonic-oscillator shell model.

Multipole	Transition	Particles	ΔE_{osc}	Fitted b (fm)	χ^2 per degree of freedom
$M6$	$0f_{7/2} \rightarrow g_{9/2}$	p,n	$1\hbar\omega$	1.419±0.009	6.5
$M6^*$	$0d_{5/2} \rightarrow 0f_{7/2}$	p	$1\hbar\omega$	1.602±0.011	14.6
$M6$	$0f_{7/2} \rightarrow 1d_{5/2}$	p,n	$1\hbar\omega$	a	
$M7$	$0f_{7/2} \rightarrow 0h_{11/2}$	p,n	$2\hbar\omega$	1.556±0.009	1.0
$M8$	$0f_{7/2} \rightarrow 0g_{9/2}$	p,n	$1\hbar\omega$	1.860±0.010	1.2
$M9$	$0f_{7/2} \rightarrow 0h_{11/2}$	p,n	$2\hbar\omega$	1.976±0.010	4.7
$M10$	$0f_{7/2} \rightarrow 0i_{13/2}$	p,n	$3\hbar\omega$	2.087±0.010	14.6

[a]For reasonable values of b, the calculated form factor has a dip in the vicinity of the experimental maximum.

$$F_T^2(q) = \text{const} \times q^{2J} \exp(-b^2 q^2/2) , \quad (7)$$

where J is the multipole order. The validity of the use of the harmonic oscillator model and q_{eff} in the analysis of electroexcited stretched states has been discussed previously.[4]

Initially, all data were fitted to $M8$ form factors calculated for a $0f_{7/2} \rightarrow 0g_{9/2}$ single-particle transition, with equal and opposite neutron and proton amplitudes, i.e., an isovector transition. Since the same value of b is used for the neutron and proton contributions, the shape of the resulting form factor is independent of the relative neutron and proton contributions assumed. The oscillator length parameter b and the normalization for an assumed pure isovector transition $\tilde{Z}_1^2$ were varied in each fit. For the reasons discussed above, only the 154° data were used in the fits. $\tilde{Z}_1^2$ corresponds to the effective value of the isovector spectroscopic strength discussed following Eq. (11). For the two strongest high-multipolarity states observed, those at 15.47 and 8.10 MeV, the best $M8$ fit was obtained for oscillator parameters of 1.860±0.010 fm and 1.840±0.024 fm, respectively, close to the value of $b = 1.90 \pm 0.02$ fm obtained for $M8$ transitions in ^{54}Fe.[11] They also agree well with the expected value of the oscillator parameter for the $0f_{7/2}$ subshell based on the rms radius of the subshell as obtained from magnetic elastic electron scattering.[14,20] Using the harmonic-oscillator shell model relation

$$\langle r^2 \rangle_{nl} = (2n + l + 3/2) b^2 ,$$

where n ($=0,1,\ldots,$) and l are the radial and orbital quantum numbers, the data[14] imply $b(0f_{7/2}) = 1.879 \pm 0.025$ and 1.889±0.023 fm for neutrons and protons, respectively.

To confirm the $M8$ identification of these states, fits to other multipoles were also performed, as indicated in Table I. The next highest multipole attainable via a $1\hbar\omega$ excitation is $M6$, which, like $M8$, can occur as a $0f_{7/2} \rightarrow 0g_{9/2}$ transition. When the strong state at 15.47 MeV was fit to this configuration, the required value of b was 1.419±0.009 fm, an unreasonably small value. Because of the four proton holes in the $0f_{7/2}$ shell in the ^{52}Cr ground state, an $M6$ excitation may also be produced by a $0d_{5/2} \rightarrow 0f_{7/2}$ proton transition, ($M6^*$), which, however, can excite only $T = 2$ states. With this configuration used in the fit, $b = 1.602 \pm 0.011$ fm, still unreasonably small. Although the b value obtained for the $M9$ fit in Table I is not *a priori* unreasonable, it would require a $2\hbar\omega$ excitation, whose strength should be distributed at higher excitation energies than those measured here ($\hbar\omega = \hbar^2/M_p b^2 \simeq 12$ MeV). In view of the observed concentration of high-multipole excitations between 8 and 16 MeV with consistent form factor shapes, it is reasonable to conclude that the 8.10 and 15.47 MeV states are in fact the strongest of the 8^- states sought by this experiment.

In order to determine multipolarity of the weaker excitations, the oscillator length parameter was fixed at 1.860 fm, and form factors calculated for the various configurations of Table I were fitted to the data for each level with only the normalization varied. Figure 4 shows the shapes of the F_T^2 curves for several of these multipoles together with the data for the 15.47 MeV level.

On the basis of the χ^2 values of the various fits, the multipolarity of each level was assigned. If the χ^2 values of two fits of different multipolarity differed by less than

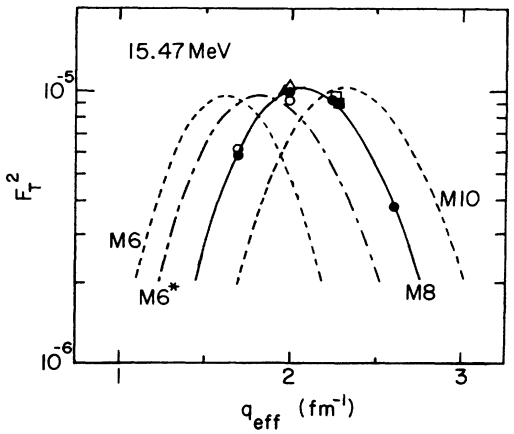

FIG. 4. Transverse form factor squared for the 15.47 MeV level, together with harmonic-oscillator shell model fits to various multipoles with $b = 1.860$ fm, as described in the text. The data point symbols have the same meaning as in Fig. 2.

1, the assignment was considered ambiguous. A few levels with large χ^2 or with qualitatively unconvincing form factors were identified as "uncertain" $M8$'s. Of the 35 observed high-multipolarity transverse excitations, 18 were identified as unambiguous $M8$'s, and nine as $d_{5/2}\rightarrow f_{7/2}$ $M6$'s. The $f_{7/2}\rightarrow g_{9/2}$ $M6$ assignment was preferred for only one level, 13.57 MeV, and no reasonable candidates for $M7$ or $M9$ were found. Table II presents the results of the fits. The uncertainty in the excitation energy is 20 keV. The list of "$M6$" transitions in the table is neither definitive nor exhaustive, and no further analysis of these states was undertaken.

IV. RESULTS

The strength of each $M8$ excitation in Table II is expressed in terms of the effective isovector spectroscopic amplitude $\tilde{Z}_1^2$ defined in Sec. III. The uncertainty in $\tilde{Z}_1^2$ does not include the 5% systematic uncertainty in the normalization of the cross section. The strength distribution is plotted in the upper part of Fig. 5. The experiment indicates that the $M8$ strength in ^{52}Cr consists of one very strong state at 15.47 MeV, moderately strong states at 8.10, 9.65, 11.27, and 11.96 MeV, and a large number of weaker states. This is qualitatively similar to the strength distribution[11] in ^{54}Fe. A large complex of closely spaced states is seen in the 11–12 MeV region. While not every state is clearly resolved in every spectrum, there is no doubt that the predominant strength in this region is $M8$, and that the sum of the strengths of the states in Table II gives a good representation of the total experimental $M8$ strength between 11 and 12 MeV.

Also included in Table II are the reduced transition strengths $B(M8\uparrow)$, where the upward arrow indicates a

TABLE II. Results of fitting the experimentally measured form factors with $M8$ and $M6$ transition form factors calculated for single-particle transitions in the harmonic-oscillator shell model with $b=1.860$ fm. Levels whose χ^2 values in column 2 are enclosed in parentheses have ambiguous or doubtful $M8$ assignments. $\tilde{Z}_1^2$ is the effective isovector spectroscopic strength.

	Fits to $M8$				$M6$
E_x (MeV)	χ^2 per degree of freedom ($M8$)	$10^3\times\tilde{Z}_1^2$	Statistical % error in $\tilde{Z}_1^2$	$10^{-10}\times B(M8\uparrow)$ (μ_N^2 fm^{14})	χ^2 per degree of freedom ($M6$)
8.10	2.8	20.69	2.4	27.53	
8.45					1.5
8.94	(4.8)	5.92	6.9	7.86	(6.2)
9.08	(2.0)	7.99	5.6	10.62	
9.45	2.4	9.22	4.8	12.26	
9.66	6.1	13.13	3.8	17.44	
9.91	1.0	8.22	5.8	10.92	
10.11	(7.0)	7.92	6.2	10.52	
10.33					3.1
10.51	(4.3)	5.04	9.7	6.70	(3.7)
10.80	(3.1)	7.73	6.2	10.24	(3.0)
11.00	1.4	4.29	11.4	5.70	
11.17	0.5	4.92	10.3	6.52	
11.27	3.8	19.04	3.2	25.25	
11.39	1.0	4.71	11.1	6.25	
11.55	0.8	4.48	11.7	5.95	
11.66	0.6	7.54	7.2	9.99	
11.77	1.0	9.12	6.2	12.08	
11.88	0.9	10.33	6.1	13.70	
11.96	1.7	12.95	5.3	17.17	
12.03	(1.3)	6.74	9.6	8.66	
12.13	(1.7)	6.13	9.5	8.12	(0.9)
12.24					0.5
12.73	2.7	8.28	7.0	10.96	
13.22	2.1	7.76	7.2	10.27	
13.39					2.8
13.57					0.8
13.71					1.7
14.03					5.3
14.34					0.2
14.43	0.8	5.93	10.8	7.84	
15.27					5.8
15.47	1.2	101.41	1.0	133.74	
16.40					2.7
16.69	(2.1)	7.13	11.7	9.39	

transition from the ground state to the excited state. Unlike the $\tilde{Z}_1^2$ values, which are relatively insensitive to the value of the oscillator parameter b used in the fits, the $B(M8\uparrow)$ are very model dependent since they are proportional to b^{14} and imply an extrapolation in momentum transfer from the measured region down to the photon point.

V. THEORETICAL CALCULATIONS

In order to interpret the fragmentation and isospin splitting of the $M8$ strength, we have compared the experimental results to shell model calculations equivalent to those described previously.[11] In the even $f_{7/2}$-shell nuclei the ground state is assumed to be described by the configuration $(f_{7/2}^n)_{J=0}^T$, where n is the number of nucleons and T is the isospin. The stretched 8^- states arise from promoting an $f_{7/2}$ particle to the $g_{9/2}$ orbit and are described by the configurations

$$[(f_{7/2}^{n-1})_{J'}^{T'} \times g_{9/2}]_{J=8}^{T_f} ,$$

where J' is half-integral and can take on all values consistent with the exclusion principle between $\frac{7}{2}^-$ and $\frac{25}{2}^-$, $T'=T\pm\frac{1}{2}$, and, for a target nucleus with $T_z=T$, $T_f=T$ or $T+1$. With these assumptions the stretched configuration $M8$ form factors are

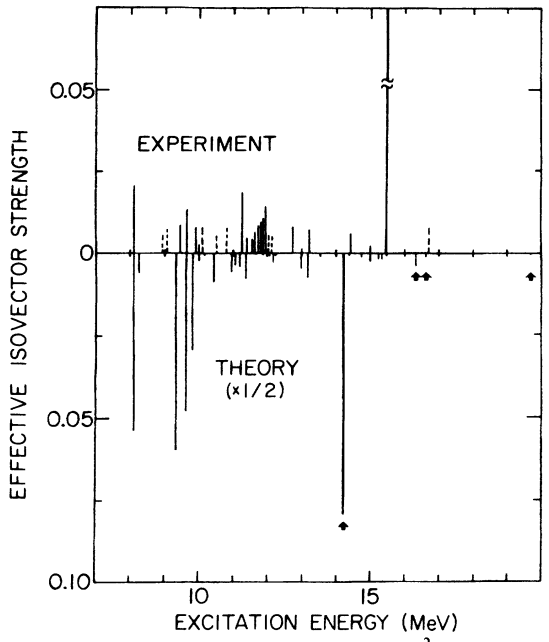

FIG. 5. Effective isovector $M8$ strengths $\tilde{Z}_1^2$, as defined in the text. The upper portion shows the results of this experiment, with the dashed lines representing levels whose $M8$ assignment is doubtful. The lower portion shows the results of the $f_{7/2}\rightarrow g_{9/2}$ shell model calculation multiplied by 0.5. The arrows denote states with $T=3$; all the other states have $T=2$. The energies of all calculated states have been shifted so that the yrast $T=2$ state is aligned with the lowest experimental level at 8.10 MeV.

$$F_{T\rightarrow T}^2=\left|\alpha\left[\frac{n+2T+2}{2(2j_b+1)(2T+1)T}\right]^{1/2}[TM_0+T_zM_1]-\beta\left[\frac{n-2T}{2(2j_b+1)(2T+1)(T+1)}\right]^{1/2}[(T+1)M_0-T_zM_1]\right|^2 , \quad (8)$$

$$F_{T\rightarrow T+1}^2=\left|\gamma\left[\frac{n-2T}{2(2j_b+1)(T+1)}\right]^{1/2}M_1\right|^2 , \quad (9)$$

where, for ^{52}Cr, $T_z=T=2$ and $n=12$. M_0 and M_1 are the isoscalar and isovector matrix elements, which include nucleon size and center-of-mass corrections. Their ratio[21] is

$$\frac{M_0}{M_1}=\frac{(\mu_n+\mu_p)}{(\mu_n-\mu_p)}=-0.187 . \quad (10)$$

The numerical value on the right-hand side of this equation assumes that the nucleon magnetic moments μ_n and μ_p have their free-particle values, $-1.91\ \mu_N$ and $2.79\ \mu_N$, respectively. In Eq. (8), α^2 is the probability of the configuration

$$[(f_{7/2}^{n-1})_{J'=7/2,\nu=1}^{T'=T-1/2}\times g_{9/2}]_{J=8}^{T}$$

in the observed state, where the subscript $\nu=1$ implies the state must have seniority one. Similarly, β^2 and γ^2 are the probabilities of the configurations

$$[(f_{7/2}^{n-1})_{J'=7/2,\nu=1}^{T'=T+1/2}\times g_{9/2}]_{J=8}^{T}$$

and

$$[(f_{7/2}^{n-1})_{J'=7/2,\nu=1}^{T'=T+1/2}\times g_{9/2}]_{J=8}^{T+1} ,$$

respectively. These coefficients are obtained by diagonalizing the shell model Hamiltonian. When the $[(f_{7/2}^{11})\times g_{9/2}]_8^{T_f}$ model space is used to describe 8^- states in ^{52}Cr, 38 $T_f=2$ and four $T_f=3$ states are possible. The predicted spectrum and distribution of strengths depend upon the residual two-body interaction used in the shell model calculation. In the results presented here, the interaction is that used previously: The $(f_{7/2}^2)$ matrix elements were obtained[22] from the spectrum of ^{54}Co, and the $(f_{7/2}g_{9/2})$ residual force was calculated using the Schiffer-True potential,[23] with the oscillator parameter $b=1.86$ fm. The theoretical $M8$ results obtained from this calculation imply that nearly all (95%) of the $T\rightarrow T+1$ strength is concentrated in a single state, while 73% of the $T\rightarrow T$ strength is shared by four states of comparable strength. The remaining strength is divided among a large number of weaker transitions, as is shown

in the lower part of Fig. 5, where the energies have been adjusted so that the predicted yrast 8^-, $T=2$ state lines up with the lowest-lying experimental 8^- state at 8.10 MeV. The calculated quantity plotted in Fig. 5 is

$$Z_1^2(\text{eff})=2(Z_n\mu_n+Z_p\mu_p)^2/(\mu_n-\mu_p)^2 , \quad (11)$$

which is the spectroscopic strength of a hypothetical pure isovector transition yielding the same cross section as the calculated transition, and is directly comparable with the experimentally extracted $\tilde{Z}_1^2$ plotted in the upper portion of the figure.

The model discussed in the preceding paragraphs has been called, improperly, the extreme single-particle-hole model. On the basis of the model, sum rules for the $(J=0,T)\rightarrow(J=8,T)$ and $(J=0,T)\rightarrow(J=8,T+1)$ transitions, i.e., $\Delta T=0$ and $\Delta T=1$ transitions, respectively, can be obtained, independent of the residual two-body interaction used in the calculation. For the former, the sum rule is obtained from Eq. (8) by squaring and adding the two terms with $(\alpha=1,\beta=0)$ and $(\alpha=0,\beta=1)$, and for the latter by squaring Eq. (9) and setting $\gamma=1$. The results for ^{52}Cr are

$$\sum F^2_{\Delta T=1}=\tfrac{1}{6}M_1^2 , \quad (12a)$$

$$\sum F^2_{\Delta T=0}=\tfrac{7}{12}M_1^2+\tfrac{1}{2}M_1M_0+\tfrac{3}{4}M_0^2 , \quad (12b)$$

$$\sum F^2_{\text{tot}}=\tfrac{3}{4}M_1^2+\tfrac{1}{2}M_1M_0+\tfrac{3}{4}M_0^2 . \quad (12c)$$

Corresponding to each of the three cases of Eq. (12), we may define effective isovector spectroscopic sums with the use of Eq. (10),

$$Z^2_{>}=\sum Z_1^2(\text{eff})_{T\rightarrow T+1}=\sum F^2_{\Delta T=1}/M_1^2=\tfrac{1}{6} , \quad (13a)$$

$$Z^2_{<}=\sum Z_1^2(\text{eff})_{T\rightarrow T}=\sum F^2_{\Delta T=0}/M_1^2=0.5161 , \quad (13b)$$

$$Z^2_{\text{tot}}=\sum Z_1^2(\text{eff})=\sum F^2_{\text{tot}}/M_1^2=0.6827 , \quad (13c)$$

which are, respectively, proportional to the summed $\Delta T=1$, $\Delta T=0$, and total $M8\uparrow$ strength in the ESPHM. The reason for this normalization is that the $Z_1^2(\text{eff})$ parameters can be compared directly with the data. Note that if we neglect M_0 relative to M_1, Eqs. (13a)–(13c) become

$$Z^2_{>}=\tfrac{1}{6},\quad Z^2_{<}=\tfrac{7}{12},\quad Z^2_{\text{tot}}=\tfrac{3}{4} , \quad (14)$$

which differ only slightly. We shall now compare experiment and theory quantitatively.

VI. COMPARISON OF EXPERIMENT WITH THEORY

A. The 15.47 MeV state

In previously measured $T\neq 0$ nuclei, the $\Delta T=1$ part of the stretched high-spin strength is concentrated in a single level, which exhausts a substantial fraction of the isovector sum rule. The $T=3$ analog of the ^{52}V ground state has been assigned at an excitation energy[16] of 11.26 MeV in ^{52}Cr and an 8^- state was identified[24] at an excitation energy of 4.32 MeV in the ^{50}Ti$(\alpha,d)^{52}$V reaction. Moreover, in the ^{51}V$(t,d)^{52}$V reaction, $l=4$ was observed[25] in the transition to this state. Since the analog state has the requisite particle-hole configuration, it is reasonable to expect the yrast $T=3$, 8^- state at an excitation energy of approximately 15.58 MeV in ^{52}Cr. It therefore appears that one can, with some certainty, assign $T=3$ to the state at 15.47 MeV excitation.

In the reviews,[3,4] the strength of the strongest $T+1$ stretched state is expressed by the ratio to the $\Delta T=1$ ESPHM sum rule,

$$S^2_{>}(\text{ESPHM})=\tilde{Z}_1^2(\text{exp})/Z^2_{>}(\text{ESPHM}) ,$$

which varies from 0.18 (for the 13.26 MeV 8^- state in ^{58}Ni) to 0.56 (for the 12^- and 14^- states in ^{208}Pb). For the 15.47 MeV 8^- state in ^{52}Cr, $\tilde{Z}_1^2=0.1014\pm0.0052$ (including the 5% normalization uncertainty), and $S^2_{>}(\text{ESPHM})=0.608\pm0.031$. This is the largest fraction of the $\Delta T=1$ sum rule yet observed in an electron scattering experiment, but is consistent with the systematics for 8^- transitions in the $f_{7/2}$ shell, where the addition of protons leads to increased quenching of the $\Delta T=1$ $M8$ strength.[3]

The shell model prediction of $\tilde{Z}_1^2=0.1581$ for the strong $T=3$ level is approximately 1.5 times the value found experimentally. For some nuclei, calculations performed in larger model spaces typically result in the predicted $\tilde{Z}_1^2$ being reduced by 30–40 % from the model predictions. In particular, in ^{28}Si when the 6^- model space is extended from $[(d_{5/2})^{11}\times f_{7/2}]$ to $[(d_{5/2}s_{1/2})^{11}\times f_{7/2}]$, the predicted yrast strength is decreased by almost a factor of 2.[26] However, for the 6^- states in ^{26}Mg as measured[27] in (p,p'), inclusion of the $s_{1/2}$ level still results in a factor of 2 discrepancy between theory and experiment for $\tilde{Z}_1^2$ of the yrast $T=2$ level. For ^{52}Cr, expansion of the model space to include the $p_{3/2}$ single-particle level, but still allowing only a single nucleon in the $g_{9/2}$ orbit, increases the number of $T=3$, 8^- states from 4 to 7357. No such extended calculations are available for ^{52}Cr.

In the model under discussion, three other $T=3$ states are possible. If one normalizes the energy of the yrast $T=3$ level to the 15.47 MeV state, the remaining three are predicted to lie at 17.58, 17.88, and 20.97 MeV, respectively. Data were not obtained for excitation energies above 18 MeV and, as can be seen from Table II, the only possible 8^- state seen above is 15.47 MeV level is the 16.69 MeV state. It is conceivable that this is the second $T=3$, 8^- level, but the experimental spin assignment is uncertain and, moreover, there are other $T=2$, 8^- levels predicted in this energy range. Therefore, nothing definitive can be said about the position of the second $T=3$ level.

B. The $T=2$ states

To test the $T\rightarrow T$, $M8$ sum rule, we add the $\tilde{Z}_1^2$ values of all of the states identified as 8^- in Table II, except for the $T=3$ state at 15.47 MeV. The largest uncertainty in the sum arises from the treatment of the ambiguous and doubtful $M8$ states whose χ^2 values are enclosed in parentheses in the table. As our best estimate, we include 50% of the strength of these states, and increase the uncertainty to encompass the extremes. This leads to the results

$$\tilde{Z}_1^2(\text{exp}) = 0.205\pm0.011 + (\text{all states}) = 0.151\pm0.008 + (\text{without doubtful states}) = 0.178\pm0.029 \text{ (best estimate)} . \quad (15)$$

Using the best estimate, we obtain

$$S_<^2(\text{ESPHM}) = \tilde{Z}_1^2(\text{exp})/Z_<^2(\text{ESPHM}) = 0.345\pm0.056 .$$

This agrees well with the factor 0.33 observed for the $\Delta T=0$, $M8$ strength in ^{54}Fe, and is also consistent with the observation in pion scattering[12] that the $\Delta T=0$ isovector strength is quenched more than the $\Delta T=1$ strength relative to single-particle-hole calculations, and, moreover, for $\Delta T=0$ states, the isoscalar strength is quenched much more than the isovector strength. Of course, some portion of the effect may be due to the greater fragmentation of the $\Delta T=0$ strength and the consequent difficulty in extracting peaks with small transition strength from the experimental background. A comparison of the detection threshold of the present experiment (approximately 4% of the strength of the 15.47 MeV level) with the distribution of strengths calculated in the $f_{7/2}$ model (Fig. 5), might suggest that about 10% of the total strength to $T=2$ states is being missed, but such estimates are extremely model dependent. Without a detailed calculation of the strength distribution in a larger model space, it is difficult even to estimate the size of the "quenching" predicted to result from additional fragmentation.

Since small changes in the residual two-body interaction and an increase in the size of the model space can change the individual values of Z_0 and Z_1 for almost degenerate states, the best way to compare theory and experiment may be to "bin" the value of $\tilde{Z}_1^2$ in 1-MeV intervals. In Fig. 6 the predicted values of $\tilde{Z}_1^2$, based on the shell model calculation and the use of Eq. (10), are compared with experimental values taken from Table II. In this binning we have normalized the predicted energy of the yrast 8^-, $T=2$ state to line up with the 8.1 MeV level. Clearly, too much strength is predicted below 11 MeV, while in the 11–12 MeV bin, experiment is twice as large as theory. Above 12 MeV, both theory and experiment are small. Thus, the challenge to future theoretical calculations is to account for the fractionation of the $M8$ strength into many small unobservable parts and a shift of strength into the 11–12 MeV region. Whether this can be accomplished by expanding the shell model configuration space, and perhaps changing the residual two-body interaction, is an open question.

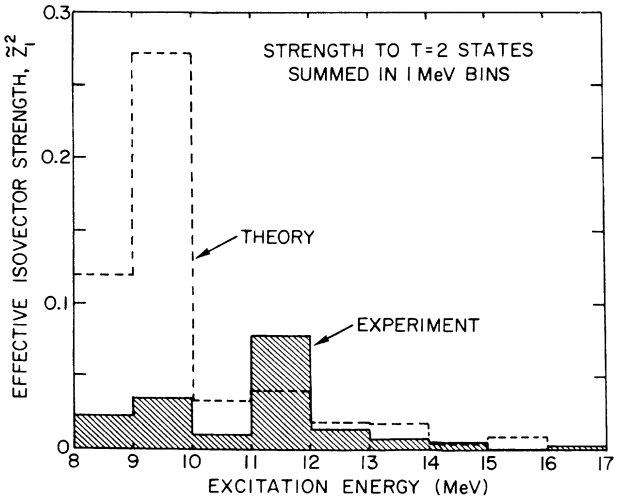

FIG. 6. $T=2$ transition strength in ^{52}Cr, summed in 1 MeV wide bins. The energies are aligned as in Fig. 5.

Finally, the effects of meson exchange currents may be estimated[28] for the present experiment, with the method of Ref. 5 which considers the contributions of the pionic and pair currents, but not those of the isobar current. Near the peak of the form factor, the exchange currents tend to increase the predicted cross sections by approximately 15%, so that correcting for mesonic effects will increase the disagreement with the ESPHM.

C. Isospin splitting

In nuclei in which the stretched magnetic strength is split into identifiable $\Delta T=0$ and $\Delta T=1$ contributions, it has been observed[29] that the difference in mean excitation energies, $\Delta\bar{E}$ frequently is consistent with a simple formula based on the Lane model[30]

$$\Delta\bar{E} = \bar{E}(T+1) - \bar{E}(T) = (T+1)V_1/A , \quad (16)$$

where A is the mass number, V_1 is an average potential energy, and the mean excitation energies are weighted by the transition strengths. For $M4$ and $M8$ transitions in six nuclei, a value[29] near 100 MeV is obtained for V_1.

For ^{52}Cr, the experimental averages are $\bar{E}(T)=11.01\pm0.05$ MeV, where the error reflects the effect of the uncertain states in Table II, and $\bar{E}(T+1)=15.47\pm0.02$ MeV. The difference, 4.46 ± 0.05 MeV, is in excellent agreement with the value of 4.50 MeV predicted by the shell model calculation. With $\Delta\bar{E}=4.46$ MeV, the Lane formula gives $V_1=77.3$ MeV, which is consistent with $V_1=73$ MeV deduced[28] from $M6$ transitions in ^{26}Mg, but inconsistent with the values (between 104 and 111 MeV) derived from stretched $M8$ excitations in ^{54}Fe, ^{58}Ni, ^{56}Fe, and ^{60}Ni.

The large number of weak $\Delta T=0$ transitions identified in the present experiment contrasts with the previous studies in which only approximately four $T_<$ states were observed. If only the four strongest observed $T=2$ states are used, the splitting is 5.38 MeV experimentally, and 5.08 MeV from the shell model calculations. Since these splittings are much closer to the values previously found, the significant difference between ^{52}Cr and its neighbors may arise from many weaker fragments that were not observed in prior experiments.

VII. CONCLUSIONS

Undoubtedly the most significant outcome of this experiment has been the excitation of the $T=3$, 8^- state at 15.47 MeV in which the entire observed $T\rightarrow T+1$ $M8$

strength is concentrated. This single transition exhausts nearly 61% of the $\Delta T=1$ sum rule based on the extreme single-particle-hole model, the largest fraction of this sum rule yet observed in an electron scattering experiment.

The fact that this fractional strength is larger than that observed in nearby nuclei may be due to the additional number of $f_{7/2}$ protons in ^{54}Fe and ^{58}Ni. This suggests a behavior similar to that of the $M1$ transitions in ^{48}Ca, ^{50}Ti, ^{52}Cr, and ^{54}Fe, where successive addition of protons to the $f_{7/2}$ shell results in increased quenching and fragmentation.[31]

All of the other observed 8^- states are deduced to have $T=2$, and thus to have both isovector and isoscalar transition strength. The observed strength of these transitions is highly fragmented, and is distributed broadly over the region of excitation energy between 8 and 13 MeV. The summed $T\rightarrow T$ strength exhausts about 35% of the ESPHM sum rule. This behavior, a single strong $T\rightarrow T+1$ transition and many fragmented $T\rightarrow T$ transitions, is consistent with that generally observed for stretched excitations in other $T\neq 0$ nuclei, as is the result that the $\Delta T=0$ isovector strength is more strongly quenched than the $\Delta T=1$ strength. A shell model calculation in the model space $[(f_{7/2})^{11}\times g_{9/2}]$ predicts extensive fragmentation of the $T\rightarrow T$ strength, but less than that observed in the experiment. Expansion of the model space would most likely bring theory into closer agreement with experiment, but such a calculation is not feasible with present techniques.

The isospin splitting of $M8$ strength, as determined by the difference in the strength-weighted averages of excitation energy for the $T\rightarrow T$ and $T\rightarrow T+1$ contributions, is 4.46 MeV. This value is in good agreement with the shell model calculation, but differs from an expectation based upon the Lane formula applied to other stretched excitations in this general mass region.

ACKNOWLEDGMENTS

We wish to thank the staff and management of NIKHEF-K for their assistance and cooperation. This work was supported by the U.S. Department of Energy, Nuclear Physics Division under Contract No. W-31-109-ENG-38, National Science Foundation Grant Nos. PHY-85-19381 and PHY-8520464, the Stichting Fundamenteel Onderzoek de Materie (FOM) with the Nederlandse Organisatie voor Zuiver Westenschappelijk Onderzoek (ZWO), and a North Atlantic Treaty Organization (NATO) Research Grant for International Cooperation.

*Present address: Naval Postgraduate School, Monterey, CA 93943.

†Present address: Stichting Energieonderzoek Centrum Nederland, Postbox 1, 1755 ZG Petten, The Netherlands.

[1]R. D. Lawson, *Theory of the Nuclear Shell Model* (Clarendon Press, Oxford, 1980).

[2]F. Petrovich and W. G. Love, Nucl. Phys. **A354**, 499c (1981).

[3]R. A. Lindgren and F. Petrovich, in *Spin Excitations in Nuclei,* edited by F. Petrovich *et al.* (Plenum, New York, 1984).

[4]R. A. Lindgren, J. Phys. (Paris) Colloq. **45**, 433 (1984).

[5]R. A. Lindgren *et al.*, Can. J. Phys. **65**, 666 (1987).

[6]F. Petrovich, J. A. Carr, and H. McManus, Annu. Rev. Nucl. Part. Sci. **36**, 29 (1986).

[7]G. F. Bertsch and I. Hamamoto, Phys. Rev. C **26**, 1323 (1982).

[8]I. S. Towner and F. C. Khanna, Nucl. Phys. **A399**, 334 (1983).

[9]L. Zybert, P. W. M. Glaudemans, R. B. M. Mooy, and D. Zwarts, Z. Phys. A **318**, 363 (1984).

[10]A. Bohr and B. Mottelson, Phys. Lett. **100B**, 10 (1981).

[11]R. A. Lindgren *et al.*, Phys. Rev. Lett. **46**, 706 (1981).

[12]D. F. Geesaman *et al.*, Phys. Rev. C **30**, 952 (1984).

[13]B. Zeidman, Argonne National Laboratory Informal Report ANL-7312, 1967.

[14]S. K. Platchkov *et al.*, Phys. Rev. C **25**, 2318 (1978).

[15]C. de Vries *et al.*, Nucl. Instrum. Methods **223**, 1 (1984).

[16]J. R. Beene, Nucl. Data Sheets **25**, 235 (1978).

[17]J. W. Lightbody, Jr. *et al.*, Phys. Rev. C **27**, 113 (1983).

[18]J. C. Bergstrom, University of Saskatchewan report, 1974 (unpublished).

[19]H. C. Lee, Chalk River National Laboratories Report AECL-4839, 1975 (unpublished).

[20]P. K. A. de Witt Huberts *et al.*, Phys. Lett. **71B**, 317 (1977).

[21]In this work the ratio M_0/M_1 and the coefficient of T_Z in Eq. (8) both have the opposite sign to those adopted in Ref. 11. With the sign convention of Ref. 11, the coefficient of M_0M_1 given in the caption of Fig. 3 of that paper should be $-\frac{1}{4}$ instead of $\frac{1}{4}$.

[22]W. Kutschera, B. A. Brown, and K. Ogawa, Riv. Nuovo Cimento **1**, 1 (1978).

[23]J. P. Schiffer and W. W. True, Rev. Mod. Phys. **48**, 191 (1976).

[24]K. Okada, J. Kawa, and T. Yamagata, Nucl. Phys. **A349**, 125 (1980).

[25]O. Karban *et al.*, Nucl. Phys. **A472**, 189 (1987).

[26]A. Amusa and R. D. Lawson, Phys. Rev. Lett. **51**, 103 (1983).

[27]R. E. Segel, *et al.* (unpublished).

[28]A. M. Lallena, J. S. Dehesa, and S. Krewald, Phys. Rev. C **34**, 322 (1986).

[29]R. A. Lindgren *et al.*, Phys. Rev. Lett. **47**, 1266 (1981).

[30]A. M. Lane, Nucl. Phys. **35**, 676 (1962).

[31]D. I. Sober *et al.*, Phys. Rev. C **31**, 2054 (1985).